# NOISE FILTERING AND ENHANCEMENT OF SEABED TOPOGRAPHY FOR AIRBORNE LASER BATHYMETRY

W. Cheng, W.-S. Lu, and A. Antoniou

Department of Electrical and Computer Engineering
University of Victoria, Victoria, B.C., V8W 3P6

**ABSTRACT**

A technique for noise filtering and enhancement of seabed topography of coastal waters is presented. The characteristics of the noise with which the bathymetric signals are contaminated are studied. A simple, yet efficient, data segmentation and interpolation method for regularizing irregularly spaced data is developed. Then a 2-D noise filtering algorithm based on the use of local statistics of depth measurements is described and applied to the data.

## I. Introduction

In airborne laser bathymetry, noise embedded in sea-depth estimates can be broadly divided into two types. The first type of noise is in the form of background noise and quantization error. This type of noise can be removed by using the 1-D signal processing techniques described in [1]. The second type of noise is noise inherent in the 2-D bathymetric profiles that is difficult to detect in individual waveforms and is, therefore, difficult to eliminate with 1-D signal processing techniques. This type of noise generally depends on the positioning of laser soundings, sea state during the survey mission, and the measurement errors of the LIDAR system. Specifically, the geographical position of each laser sounding is dependent on the laser-firing angle, aircraft position, and altitude information. In addition, transient influences such as fish shoals or floating vegetation cause incorrect reflection timing by false returns that cannot be identified by 1-D processing of a single sounding waveform. Measurement inaccuracies due to one or more of these factors contribute uncertainties in the laser-sounding location and, in turn, give rise to uncertainties in the depth estimates at the recorded geographical positions. Solving this kind of problem requires 2-D signal processing [2].

## II. Preprocessing

The depth estimated by using the algorithms developed in [1] can be viewed as a function of position coordinates, i.e.,

$$\text{Depth} = \text{F}(X,\ Y) \tag{1}$$

where $X$ is the northing coordinate and $Y$ the easting coordinate. A graphical representation of the depth function is usually desired to visualize the trend and variations of the ocean topography of the area surveyed. We can learn from Figure 1 that the laser soundings provided by the airborne laser bathymetry system discussed in this paper are distributed irregularly in a rectangular coordinate system, which may cause difficulty for some signal-processing algorithms to be applied. In what follows, we shall describe two issues that need to be considered before applying 2-D filtering for noise removal. These are data segmentation of the input data and an interpolation method to obtain regularly spaced data from irregularly spaced data.

### *A. Data Segmentation*

A survey area usually consists of thousands of soundings. In some cases, depth information is not available in the waveform received either because laser pulses from the bathymetric sensor hit a small island, in which case there is no depth to measure, or because the surveying area is too deep, too turbid, or full of ocean vegetation,



0-7803-2553-2/95/$4.00 

in which case the depth is not detectable. So before the application of 2-D filtering, it is always desirable that the useless soundings be eliminated and the data size for the 2-D signal processing be sufficiently large so that soundings at the boundary represent only a small portion of the total number of soundings being processed. This part of processing is referred to as data segmentation. The heading information such as the event number, scan number, and the coordinates of northing and easting for each waveform signal as well as the estimated depth can be used to facilitate the implementation of the data segmentation and the data interpolation discussed in the next subsection. What follows is devoted to a brief description of the heading elements that are used for data segmentation and data interpolation. An integer "event number" is assigned to each and every waveform at a survey area. The number is serial and stands for the sequence of the waveforms being collected. For the nine soundings in each arc, a "scan number" ranging from 0 to 8 is given to every waveform in the arc according to the order of the laser pulse sounding. A single waveform $x(n)$ is labeled as $x_{\mathrm{b}_i}^{\mathrm{a}_i}(n)$ to include information of the scan number, recorded as superscript $\mathrm{a}_i$, and the event number, recorded as subscript $\mathrm{b}_i$.

*B. Data Interpolation*

As mentioned above, the positions of the soundings usually exhibit an irregular pattern in a rectangular global positioning system (GPS). In addition, the boundary of a data segment is often not in parallel to the $X$ or $Y$ directions of the coordinate system. A regularization of scattered data is first formed as shown in Figure 2. Data with respect to a regular grid pattern can be obtained by the simple interpolation described below. Assuming that the $X$ and $Y$ coordinates of a grid point are given, the depth at the point can be interpolated from the depths at four other irregularly spaced points in the vicinity of the grid point by the use of a second-order bivariate polynomial. A polynomial in six terms, which comprises a constant term, two linear terms ($x$, $y$), two quadratic terms ($x^2$, $y^2$), and a cross-product term ($xy$), is used to approximate the depth data. A set of four linear equations, formed by polynomial fitting, is rearranged in matrix form.

The $X$ and $Y$ coordinates and the depths at the four points are $X(\mathrm{b}_i)$, $Y(\mathrm{b}_i)$, and $\mathrm{F}(X(\mathrm{b}_i), Y(\mathrm{b}_i))$, where $i = 1, \ldots, 4$. The $X$ and $Y$ coordinates and the depths at the grid poit of interest are denoted as $X(\mathrm{b}^*)$, $Y(\mathrm{b}^*)$, and $\mathrm{F}(X(\mathrm{b}^*), Y(\mathrm{b}^*))$. We can write

$$\begin{aligned} \mathrm{F}(X(\mathrm{b}_i), Y(\mathrm{b}_i)) &= a_0 + a_1 d_{x_i} + a_2 d_{y_i} \\ &\quad + a_3 d_{x_i}^2 + a_4 d_{y_i}^2 + a_5 d_{x_i y_i} \end{aligned} \quad (2)$$

where

$$\begin{aligned} d_{x_i} &= X(\mathrm{b}^*) - X(\mathrm{b}_i) \\ d_{y_i} &= Y(\mathrm{b}^*) - Y(\mathrm{b}_i) \\ d_{x_i y_i} &= d_{x_i} \cdot d_{y_i} \end{aligned}$$

Equation (2) can be further rearranged in matrix form as

$$\mathrm{F}(X(\mathrm{b}_i), Y(\mathrm{b}_i)) = \mathbf{D}_i \mathbf{A} \quad (3)$$

where

$$\begin{aligned} \mathbf{D}_i &= \left[1\ d_{x_i}\ d_{y_i}\ d_{x_i}^2\ d_{y_i}^2\ d_{x_i y_i}\right] \\ \mathbf{A} &= \left[a_0\ a_1\ a_2\ a_3\ a_4\ a_5\right]^T \end{aligned}$$

for $i = 1, \ldots, 4$. The four equations of (3) can be rearranged as

$$\begin{bmatrix} \mathrm{F}(X(\mathrm{b}_1), Y(\mathrm{b}_1)) \\ \mathrm{F}(X(\mathrm{b}_2), Y(\mathrm{b}_2)) \\ \mathrm{F}(X(\mathrm{b}_3), Y(\mathrm{b}_3)) \\ \mathrm{F}(X(\mathrm{b}_4), Y(\mathrm{b}_4)) \end{bmatrix} = \begin{bmatrix} 1\ d_{x_1}\ d_{y_1}\ d_{x_1}^2\ d_{y_1}^2\ d_{x_1 y_1} \\ 1\ d_{x_2}\ d_{y_2}\ d_{x_2}^2\ d_{y_2}^2\ d_{x_2 y_2} \\ 1\ d_{x_3}\ d_{y_3}\ d_{x_3}^2\ d_{y_3}^2\ d_{x_3 y_3} \\ 1\ d_{x_4}\ d_{y_4}\ d_{x_4}^2\ d_{y_4}^2\ d_{x_4 y_4} \end{bmatrix} \mathbf{A}$$

or

$$\mathcal{F} = \mathcal{D} \cdot \mathbf{A} \quad (4)$$

where

$$\mathcal{F} = \begin{bmatrix} \mathrm{F}(X(\mathrm{b}_1), Y(\mathrm{b}_1)) \\ \mathrm{F}(X(\mathrm{b}_2), Y(\mathrm{b}_2)) \\ \mathrm{F}(X(\mathrm{b}_3), Y(\mathrm{b}_3)) \\ \mathrm{F}(X(\mathrm{b}_4), Y(\mathrm{b}_4)) \end{bmatrix}$$

$$\mathcal{D} = \begin{bmatrix} 1\ d_{x_1}\ d_{y_1}\ d_{x_1}^2\ d_{y_1}^2\ d_{x_1 y_1} \\ 1\ d_{x_2}\ d_{y_2}\ d_{x_2}^2\ d_{y_2}^2\ d_{x_2 y_2} \\ 1\ d_{x_3}\ d_{y_3}\ d_{x_3}^2\ d_{y_3}^2\ d_{x_3 y_3} \\ 1\ d_{x_4}\ d_{y_4}\ d_{x_4}^2\ d_{y_4}^2\ d_{x_4 y_4} \end{bmatrix} = \begin{bmatrix} \mathbf{D}_1 \\ \mathbf{D}_2 \\ \mathbf{D}_3 \\ \mathbf{D}_4 \end{bmatrix}$$

A solution of the above set of linear equations is then obtained by applying a pseudoinverse matrix operation on the nonsquare coefficient matrix $\mathcal{D}$ [3]. We can write

$$\mathbf{A} = \mathcal{D}^{+}\mathcal{F} \tag{5}$$

where

$$\mathcal{D}^{+} = \left(\mathcal{D}^{T}\mathcal{D}\right)^{-1}\mathcal{D}^{T}$$

From (2), it can be observed the depth at the grid point of interest can be obtained directly from the first element of vector $\mathbf{A}$, i.e., $\mathrm{a}_0$. In other words,

$$\mathrm{F}\left(X\left(\mathrm{b}^{*}\right), Y\left(\mathrm{b}^{*}\right)\right) = \mathrm{a}_0$$

The interpolated depth profile can be illustrated by the contour map shown in Figure 3.

## III. Additive Noise Filtering

In this section, attention will be given to the filtering of a given 2-D profile of sea depth that has been degraded by a certain amount of noise. In [4], an algorithm for the removal of additive noise from a degraded image based on the local statistics of the image at hand was proposed. What we report here can be viewed as an application of the method proposed in [4] to 2-D profiles of sea depth. If $z_{i,j}$ is the degraded pixel $x_{i,j}$ in a given 2-D sea depth profile, then

$$z_{i,j} = x_{i,j} + w_{i,j} \tag{6}$$

where $w_{i,j}$ denotes the noise which is assumed to satisfy

$$E\left[w_{i,j}\right] = 0, \qquad E\left[w_{i,j}w_{k,l}\right] = \sigma^2\delta_{i,k}\delta_{j,l} \tag{7}$$

where $\delta_{i,k}$ is the Kronecker delta function and $E$ is the expectation operator. It is also assumed that the signal $x_{i,j}$ is independent of $\omega_{i,j}$. The problem is to estimate $x_{i,j}$, given $z_{i,j}$ and the noise statistics. Under these circumstances, we can compute

$$\overline{x}_{i,j} \underline{\underline{\triangle}} E\left[x_{i,j}\right] = E\left[z_{i,j}\right] = \overline{z}_{i,j} \tag{8}$$

and

$$Q_{i,j} \underline{\underline{\triangle}} E\left[\left(x_{i,j} - \overline{x}_{i,j}\right)^2\right] = E\left[\left(z_{i,j} - \overline{z}_{i,j}\right)^2\right] - \sigma^2 \tag{9}$$

Like many filtering techniques, the mean and variance of $x_{i,j}$, which are denoted by $\bar{x}_{i,j}$ and $\bar{Q}_{i,j}$ in (8) and (9), are computed using the data in a $7\times 7$ window centered at position $(i,j)$. The noise variance $\sigma^2$ can be estimated using data $x_{i,j}$ in a flat region. Using a least-squares approach, we seek to find an optimal unbiased linear estimate of $x_{i,j}$, i.e.,

$$\hat{x}_{i,j} = k_{i,j}z_{i,j} + c_{i,j} \tag{10}$$

such that

$$E\left[\hat{x}_{i,j}\right] = \bar{x}_{i,j} \tag{11}$$

and

$$J = E\left[\hat{x}_{i,j} - x_{i,j}\right]^2 \tag{12}$$

is minimized. To meet condition (11), $c_{i,j}$ must satisfy

$$c_{i,j} = \hat{x}_{i,j}\left(1 - k_{i,j}\right)$$

which leads (10) to

$$\hat{x}_{i,j} = (1 - k_{i,j})\overline{x}_{i,j} + k_{i,j}z_{i,j} \tag{13}$$

By using (12) and (13) to solve $\partial J/\partial k_{i,j} = 0$, we obtain

$$k_{i,j} = \frac{Q_{i,j}}{Q_{i,j} + \sigma^2} \tag{14}$$

Since $Q_{i,j}$ and $\sigma^2$ are both positive, $k_{i,j}$ will lie between 0 and 1. It follows from (14) that for a low signal-to-noise ratio region $Q_{i,j}$ is small compared with $\sigma^2$, $k_{i,j} \simeq 0$, and the estimated $\hat{x}_{i,j}$ is $\overline{x}_{i,j}$. On the other hand, for a high signal-to-noise ratio region, $Q_{i,j}$ is much larger than $\sigma_1^2$, $k_{i,j} \approx 1$, and $\hat{x}_{i,j} \approx z_{i,j}$. The use of different window sizes greatly affects the quality of processed images. If the window is too small, the noise filtering algorithm is not effective. If the window is too large, subtle details of the image are lost in the filtering process. As reported in [4] a window size of $7 \times 7$ usually leads to satisfactory processing results. The filtered version of the profile of Figure 3 is shown in Figure 4.

## IV. Conclusion

A method for the regularization of 2-D bathymetric data has been implemented using data segmentation and interpolation. The method is straightforward and enables the processing of the data by linear or nonlinear

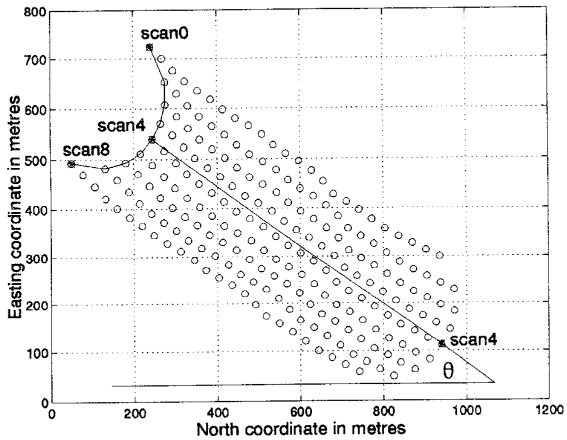


Figure 1: Scattering sounding pattern, each circle corresponds to a sounding.

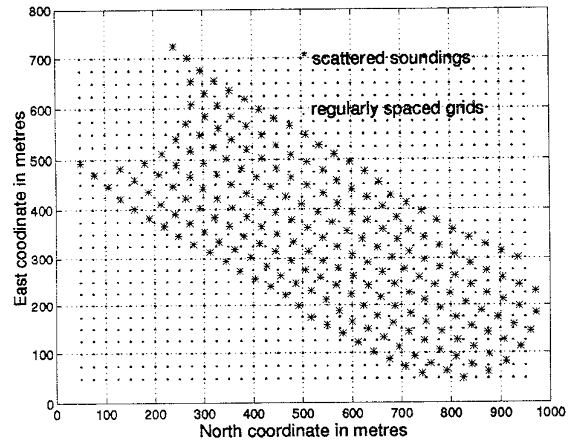


Figure 2: Formation of regularly spaced data.

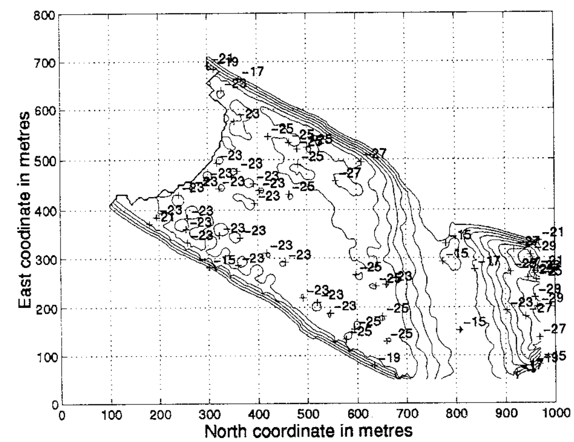


Figure 3: Contour map of reconstructed seabed topography by interpolation.

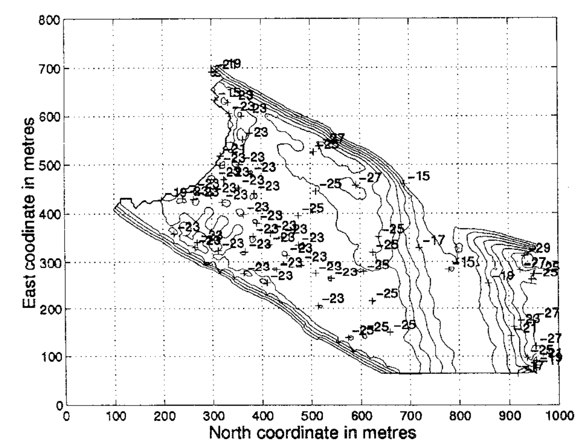


Figure 4: Contour map of filtered topography, window size $7 \times 7$, noise variance 0.09.

filters. A noise filtering technique by the use of local statistics has then been applied to preprocess the data. The outcome is a smoother profile in which wideband noise is removed.

### Acknowledgement

The authors are grateful to the Natural Sciences and Engineering Research Council of Canada and Micronet, NCE Program, for supporting this research.

### References

[1] W. Cheng, W.-S. Lu, and A. Antoniou, "Efficient waveform decomposition for airborne laser bathymetry," *IEEE Pacific Rim Conference on Communications, Computers, and Signal Processing*, Victoria, B.C., May 17-19, 1995.

[2] W.-S. Lu and A. Antoniou, *Two-Dimensional Digital Filters*, New York, Marcel Dekker, 1992.

[3] D. S. Watkins, *Fundamentals of Matrix Computations*, Wiley, pp. 420-421, 1991.

[4] J.-S. Lee, "Digital image enhancement and noise filtering by use of local statistics," *IEEE Trans. Pattern Anal. and Machine Intelligence*, vol. 2, no. 2, pp. 165-168, March 1980.